

# Hybrid superabsorbent polymer networks (SAPs) encapsulated with SiO<sub>2</sub> for structural applications

Irene Kanellopoulou, Evangelia K. Karaxi, Anna Karatza, Ioannis A. Kartsonakis, and Costas Charitidis\*

National Technical University of Athens, School of Chemical Engineering, RNANO Lab – Laboratory of Advanced, Composite, Nanomaterials and Nanotechnology, 9 Heroon Polytechniou str., Zografou Campus, 15773, Athens, Greece

**Abstract.** In this work, materials that as additives in cement promote self-sealing/healing properties by the gradual release of water they absorb were synthesized, characterized and evaluated. Specifically, hybrid SAPs that absorb high amounts of water encapsulated with SiO<sub>2</sub> that facilitates their incorporation in the matrix since it improves their chemical affinity were investigated. The structure and morphology of the fabricated SAPs were characterized analytically and confirmed the synthesis of P(MAA-co-EGDMA)@SiO<sub>2</sub> nanocomposite. Its particle size is expected to reduce the size of the pores formed due to the absorbing/desorbing water process during the mixing and curing of cement. Moreover, the water absorbance of the above mentioned material as well as its ability to maintain its original structure during subsequent cycles of absorbing/desorbing water from different mediums and specifically from distilled water (DW) and cement slurry filtrate (CS) were evaluated. CS was chosen to mimic the cementitious environment considering the presence of various ions and its pH value (~ 12). The results revealed that the absorption ratio of P(MAA-co-EGDMA)@SiO<sub>2</sub> in DW and CS was higher than 1500 wt.% its original dry weight, while SEM pictures proved that the hybrid SAPs maintained their structure after the water absorption tests.

## Introduction

Superabsorbent polymers (SAPs) are partially crosslinked, three-dimensional (3D) polymer networks which can retain water from aqueous solutions in huge amounts due to their hydrophilic nature. The water retained by SAPs can be up to thousands of times their own dry weight [1-3]. Their hydrophilic nature is owed to hydrophilic groups incorporated in the polymer structure. The swollen state of SAPs is known as hydrogels which can also demonstrate a reversible behaviour by de-swelling. Hydrogels maintain the initial 3D structure of SAPs and are not dissolved in water basically due to their crosslinking [4, 5]. Hydrogels are widely used in hygienic products, agriculture, drug delivery systems, sealing,

---

\* Corresponding author: [charitidis@chemeng.ntua.gr](mailto:charitidis@chemeng.ntua.gr)

pharmaceuticals, biomedical applications, tissue engineering, biosensors etc [5]. Both swelling and deswelling behaviour of hydrogels highly depend on their architecture. Therefore, several modifications on the design of the polymeric molecules have been investigated and the corresponding results have been reported [4]. For instance, rapid kinetics are favoured by decreased molecule size and the incorporation of micro porosity on the polymer surface increases the contact area between the hydrogel and the solvent [4].

Recently, interesting applications of hydrogels in construction and more specifically in cementitious materials have been investigated. SAPs in concrete reduce autogenous shrinkage and form a novel approach to limit cracking. This effect is realized through the gradual release of water during cement setting and hardening thus promoting a self-curing functionality through  $\text{CaCO}_3$  precipitation [6, 7]. Nevertheless, the lack of adhesion between the phases of the cement additives and the SAPs could result in failure of the interface. Moreover, one of the greatest challenges regarding the SAPs/cement composites is the process which is followed for their incorporation in the concrete mix as well as the decrement in the mixture's workability. More specifically, the SAPs should retain their ability to absorb and release water after and during a crack formation. Consequently, a self-healing/sealing effect will also ideally take place during water absorption and swelling of the cross-linked polymer network. Additionally, the absorbing/desorbing behaviour of SAPs during and after the mixing procedure, respectively, is responsible for the macro-pores formation in the produced specimens and the deterioration of their mechanical properties. The motivation of the present work is to counterbalance the abovementioned drawbacks by the introduction of materials with increased compatibility with the cement-based matrix that will exhibit high water absorption capacity and keep their morphology and structure in conditions that mimic the cement environment [3, 6, 7].

The aim of this work is to fabricate SAPs in the sub-micron to nano-scale, of enhanced chemical affinity to cement that reveal chemical stability, high water absorbency and reversible absorption/desorption behaviour in ionic solutions, all properties relevant to the SAPs expected behaviour as additives in cement admixtures to promote self-sealing/healing and reduce autogenous shrinkage during and after mixing of cement [8].

In this study, hybrid organic core-inorganic shell SAPs were synthesized by the copolymerization of Methacrylic Acid (MAA) with Ethylene Glycol Dimethacrylate (EGDMA), followed by chemical modification of the carboxyl groups with NaOH thus enhancing SAPs hydrophilicity, while the subsequent encapsulation of the modified copolymer with  $\text{SiO}_2$  inorganic shell led to the production of  $\text{P(MAA-co-EGDMA)}@ \text{SiO}_2$  nanocomposites. The SAPs encapsulated with the  $\text{SiO}_2$  inorganic shell showed immense improvement in water absorbency in both distilled water and cement slurry filtrate (ionic solution that mimics the conditions in cement) and at the same time proved to maintain their structure after absorption/desorption tests in both mediums as shown in the corresponding SEM images. Moreover, they are expected to reveal enhanced chemical compatibility with cement due to the  $\text{SiO}_2$  shell and to reduce the size of the pores formed in cement during and after the mixing procedure because of the absorbing/desorbing behaviour of SAPs, due to their small size and narrow size distribution.

## 1 Experimental

### 1.1 Materials

Methacrylic acid (MAA, from Acros Organics) as ionic monomer distilled before use. 1,2-ethanediol dimethacrylate (EGDMA, 98% stabilized) was also obtained from Acros Organics. Potassium persulfate (KPS, from Merck, extra pure) as an initiator soluble in

acetonitrile, acetonitrile (ACN, from Sigma Aldrich, ultra min 99%) as solvent, Sodium Hydroxide (NaOH, from Lachiner, 99.5%) as ionization medium, tetraethyl orthosilicate (TEOS from Fluka,  $\geq 99\%$ ) as the precursor for SiO<sub>2</sub> shell formation via sol-gel technique and ammonium hydroxide (from Sigma Aldrich, analytical grade) as pH buffer solution.

## 1.2 Synthesis of hybrid super absorbent polymer networks, SAPs

The synthesis of the hybrid SAPs is consisted of three steps: (i) preparation of the SAPs based on the copolymerization of MAA with EGDMA, (ii) ionization of the synthesized SAPs and (iii) encapsulation of the synthesized SAPs in SiO<sub>2</sub> shell.

### (i) Preparation of the SAPs

P(MAA-co-EGDMA) sub-micron spheres were prepared by radical polymerization in ACN. The polymerization took place in a 1 L-reactor equipped with a condenser under inert atmosphere (nitrogen, N<sub>2</sub>, flow) at 80°C with constant and vigorous stirring. ACN (800 mL) was added in the reactor vessel and vigorous stirring began. The reaction proceeded under N<sub>2</sub> flow for about half an hour to discard oxygen remains from the reaction vessel when at the same time temperature was set at 80°C. When the temperature reached the set point, first the distilled MAA (21 mL) and then EGDMA (2.7 mL) were added in the reactor dropwise. Finally, the initiator, KPS (0.7 g) which was previously dissolved in a small amount of ACN (~ 5 mL) using an ultrasonic bath was supplied in the reaction mixture in the same manner and the polymerization reaction continued overnight. The polymer was centrifuged at 7000 rpm for 10 minutes and then washed with ACN twice. P(MAA-co-EGDMA) spheres were stored in paste form in ACN.

### (ii) Ionization of the synthesized SAPs

Around 12 g of P(MAA-co-EGDMA) paste were dispersed in 600 mL ACN in a big beaker under magnetic stirring. 2.44 g of NaOH was then dissolved in 2-3 mL of distilled water in an ultrasonic bath and was added to the PMAA solution. The reaction continued overnight and the product was centrifuged at 7000 rpm for 10 minutes and then washed with ACN twice. The ionized P(MAA-co-EGDMA) spheres (P(MAA-co-EGDMA)-NaOH) were stored as a paste in ACN.

### (iii) encapsulation of the synthesized SAPs in SiO<sub>2</sub> shell

P(MAA-co-EGDMA)-NaOH paste (6.5 – 7 g) was dissolved in approximately 100 mL ACN using an ultrasonic bath and then the solution was supplied in the rest of the ACN (900 mL) which was placed in a big beaker under vigorous stirring. The mixture was left under stirring overnight in order to disperse any agglomerates of the P(MAA-co-EGDMA)-NaOH spheres. TEOS (42 mL) was added in the mixture dropwise and the reaction continued overnight. The product (P(MAA-co-EGDMA)@SiO<sub>2</sub>) was received after centrifugation at 5000 rpm for 5 minutes / washing with ACN twice and stored as a dry pulverized powder.

## 1.3 Instrumental Analysis

SEM (Scanning Electron Microscopy) was utilized to characterize the structure, shape and size of the SAPs prior and after swelling. SEM characterization was performed using a Phillips Quanta Inspect (FEI Company) microscope, QUANTA 200 with W (tungsten) filament 25 kV equipped with EDAX GENESIS (AMETEX PROCESS & ANALYTICAL INSTRUMENTS). All the samples were coated with gold before SEM observation. Thermogravimetric analysis (TGA) of synthesized hydrogels were performed using Polymer Laboratories systems at a heating rate of 20 °C/min under nitrogen atmosphere.

Additional data concerning the structure of the produced SAPs and the composition of their surface coating were obtained by TEM (Transmission Electron Microscopy) observations which were carried out in a JEM2000 FX (200KV, resolution 0.28 nm).

The functional groups of the specimens were characterized by FTIR (equipped with an Attenuated Total Reflectance module with a diamond crystal)) using an Agilent Cary 630 spectrometer. FTIR spectroscopy measurements were performed on as-produced vacuum dried pulverized specimens.

Thermogravimetric analysis (TGA) of the synthesized hydrogels was performed using NETZSCH STA 449 FS Jupiter system at a heating rate of 5°C/min in nitrogen atmosphere in the range of 20 to 600°C.

## 1.4 Absorption ratio measurements

To determine absorption ratio (AR) of SAPs ( $gg^{-1}$ ) weighed amounts of vacuum dried pulverised SAPs ( $M_1$ ) and excess of distilled water (DW) and cement slurry filtrate (CS) were added in eppendorfs. CS was produced to mimic the environment inside the concrete (high pH and presence of ions). Specifically, a cement solution was prepared by mixing 10 g cement (CEM I 42.5R, Lafarge) with 100 mL tap water. The cement slurry was first mixed for 1 h and then was filtered. The CS pH value was determined by pH indicator paper around 12 [9].

At specific time intervals (5, 10, 15, 20, 30, 60 minutes and one day) the SAPs were centrifuged at 15.000 rpm for 5 minutes, the supernatant liquid was rejected and the SAPs were weighed again ( $M_2$ ). The absorption ratio (AR%) was calculated using the following equation. Creation of the hydrogel was in all cases instantaneous.

$$AR\% = [(M_2 - M_1) / M_1] \times 100 \quad (1)$$

## 2 Results and Discussion

### 2.1 Instrumental Analysis

SEM: Figure 1 shows SEM images of the as-synthesized P(MAA-co-EGDMA) (1a), P(MAA-co-EGDMA)-NaOH (1b) and P(MAA-co-EGDMA)@SiO<sub>2</sub> (1c).

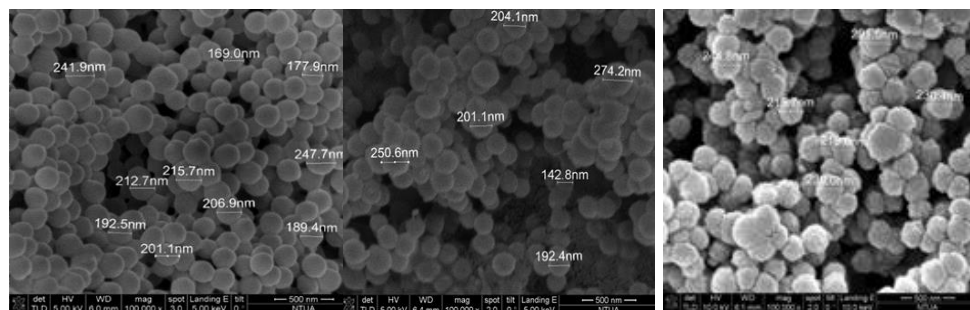


**Fig. 1a.** P(MAA-co-EGDMA) (x100.000)

**Fig. 1b.** P(MAA-co-EGDMA)-NaOH (x100.000)

**Fig. 1c.** P(MAA-co-EGDMA)@SiO<sub>2</sub> (x100.000)

Figure 2 shows SEM images of P(MAA-co-EGDMA) (2a), P(MAA-co-EGDMA)-NaOH (2b) and P(MAA-co-EGDMA)@SiO<sub>2</sub> (2c) after the water absorption tests.

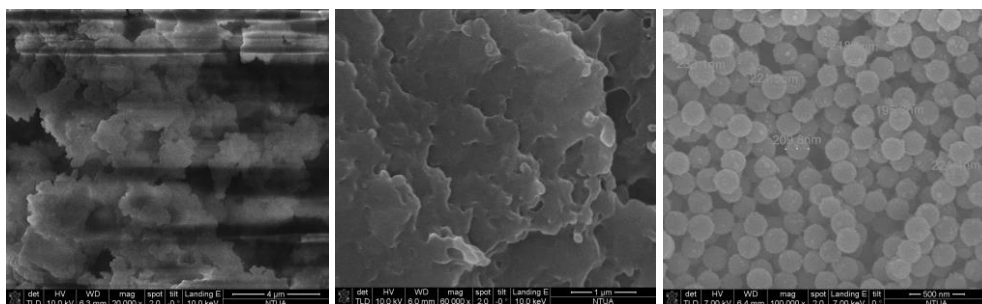


**Fig. 2a.** P(MAA-co-EGDMA) (x 20.000) after water absorption tests

**Fig. 2b.** P(MAA-co-EGDMA)-NaOH (x40.000) after water absorption tests

**Fig. 2c.** P(MAA-co-EGDMA)@SiO<sub>2</sub> (x20.000) after water absorption tests

From these images it is observed that the synthesized SAPs have a uniform structure. They are spherical and their size lies in the submicron area, while they maintain their shape and size during all the synthesis steps (ionization and encapsulation in the SiO<sub>2</sub> shell). Moreover, only the hybrid organic core – inorganic shell SAPs, P(MAA-co-EGDMA)@SiO<sub>2</sub>, maintains its structure (shape and size) after the water absorption tests.

According to SEM-EDAX analysis only the submicron spheres of P(MAA-co-EGDMA)@SiO<sub>2</sub> contain silica, while oxygen and carbon concentration is reduced from P(MAA-co-EGDMA) to P(MAA-co-EGDMA)@SiO<sub>2</sub> thus proving the successful encapsulation of the polymeric core in the inorganic shell. These results are presented in Table 1.

**Table 1.** SEM-EDAX analysis for carbon, oxygen and silicon in P(MAA-co-EGDMA) and P(MAA-co-EGDMA)@SiO<sub>2</sub> samples.

Sample	C		O		Na		Si	
	wt %	at %	wt %	at %	wt %	at %	wt %	at %
P(MAA-co-EGDMA)	40.37	55.05	31.09	31.8	-	-	-	-
P(MAA-co-EGDMA)-NaOH	44.91	55.06	36.85	33.92	15.28	9.79	-	-
P(MAA-co-EGDMA)@SiO <sub>2</sub>	34.19	51.33	27.27	30.85	12.20	9.60	6.88	4.44

**TEM:** In Figures 3-5 HRTEM images of the P(MAA-co-EGDMA)@SiO<sub>2</sub> sample are presented. It can be seen that in this sample nanoparticles reveal an amorphous core - crystalline shell structure where the 0.33 nm d-spacing of the {10-11} planes of hexagonal α-SiO<sub>2</sub> (bulk value 0.334 nm) is clearly resolved. In the nanoparticles shown in Figures 3-5 the width of the shell is of the order of 10 to 13 nm, that corresponds to nearly 25-35 {10-11} SiO<sub>2</sub> planes.

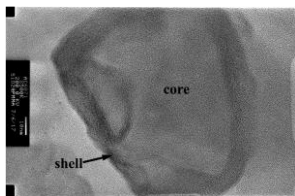


**Fig. 3.** HRTEM image of a nanoparticle with amorphous PMAA core – crystalline SiO<sub>2</sub> shell structure.

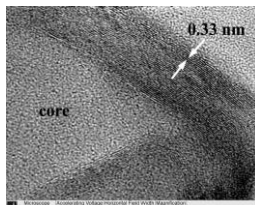


**Fig. 4.** Detail of the SiO<sub>2</sub> shell, where the {10-11} crystal planes of  $\alpha$ -SiO<sub>2</sub> are observed

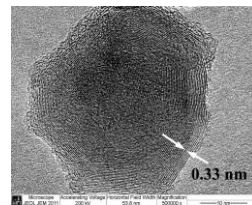


**Fig. 5.** A smaller hexagonal core-shell nanoparticle with SiO<sub>2</sub> crystalline shell, where the d-spacing of the {10-11} planes is resolved

**FTIR:** The FTIR spectra for the as-prepared, the ionized and the encapsulated SAPs are presented in Fig. 6. These spectra confirmed the formation of the inorganic shell on the polymeric core. More specifically, the spectra of only the modified spheres (P(MAA-co-EGDMA)-NaOH) and the encapsulated spheres (P(MAA-co-EGDMA)@SiO<sub>2</sub>) revealed a broad band at 3200 – 3400 cm<sup>-1</sup>, which is attributed to -OH stretching vibration due to ambient water absorbance as these molecules compared to the original P(MAA-co-EGDMA) sub-micron spheres have increased hydrophilicity. Moreover, the peaks at 1046, 782 and 445 cm<sup>-1</sup> are assigned to amorphous Si-O-Si absorbance vibrations [10, 11].

The FTIR spectra of P(MAA-co-EGDMA) and P(MAA-co-EGDMA)-NaOH displayed the characteristic absorption band of C=O vibration at 1730 cm<sup>-1</sup> which are attributed to the carbonyl groups in the MMA component [12]. Additionally, the absorption peak at 1152 cm<sup>-1</sup> was ascribed to the asymmetrical stretching of C-O in the MMA units.

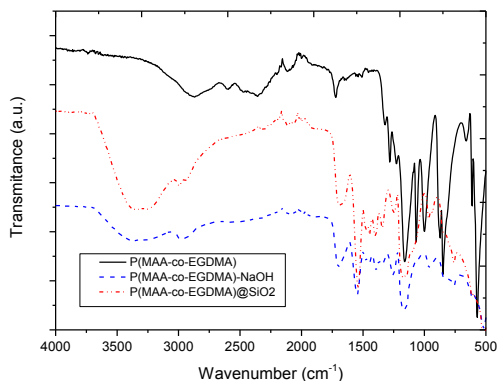


**Fig. 6.** FTIR spectra of P(MAA-co-EGDMA), P(MAA-co-EGDMA)-NaOH and P(MAA-co-EGDMA)@SiO<sub>2</sub>

The TGA of the P(MAA-co-EGDMA)@SiO<sub>2</sub> sample is illustrated in Figure 7. The first degradation process (30-180°C, 19 wt.%) is related mainly to the loss of physical absorbed water molecules through the formation of intra- and intermolecular anhydride links and acetonitrile (derived from the synthetic procedure). The second degradation step (180-300°C, 3 wt.%) is assigned to the decarboxylation of a fraction of the -COOH groups by which CO<sub>2</sub> is formed. The third and more pronounced weight loss (300-500°C, 44 wt.%), is ascribed to the complete polymer decomposition. The residual mass at 550°C corresponds to the SiO<sub>2</sub> inorganic shell and is equal to approximately 33 wt.% of the material initial mass.

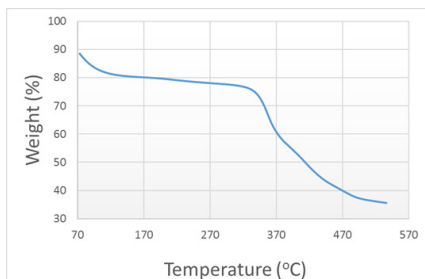


**Fig. 7.** TGA of P(MAA-co-EGDMA)@SiO<sub>2</sub>

## 2.2 Absorption ratio measurements

The SAPs AR is mainly related to the properties of the external solution such as presence of ions, charge number, ionic strength and pH value, as well as the SAPs' nature (elasticity of the network, presence of hydrophilic functional groups, and extent of crosslinking). More specifically, it is observed that SAPs AR decreases significantly in salt solutions compared to the corresponding values in distilled water, while this behaviour is mainly attributed to a "charge screening effect" of the additional ions and "ionic crosslinking" at the surface of particles in salt solutions of multivalent ions [1].

In this work, the absorption ratio (AR) of P(MAA-co-EGDMA), P(MAA-co-EGDMA)-NaOH and P(MAA-co-EGDMA)@SiO<sub>2</sub> was studied in two different mediums: distilled water, DW, (pH ~ 7) and cement slurry filtrate, CS, (pH ~ 12), which is an ionic medium that mimics the conditions in the cement environment. The AR of all SAPs is shown in Figure 8.

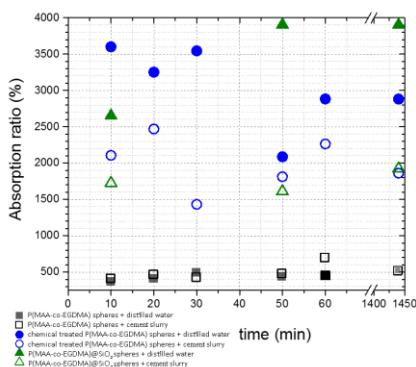


**Fig. 8.** AR% of P(MAA-co-EGDMA), P(MAA-co-EGDMA)-NaOH and P(MAA-co-EGDMA)@SiO<sub>2</sub> in distilled water and cement slurry filtrate

All SAPs synthesized, P(MAA-co-EGDMA), P(MAA-co-EGDMA)-NaOH and P(MAA-co-EGDMA)@SiO<sub>2</sub>, absorbed great amounts of water and specifically 515 g, 2880 g and 3900 g per g of dry material respectively (maximum AR values are noted for each case) thus forming hydrogels. The absorption capacity of these SAPs in DW and CS followed a similar trend as the amount of water absorbed was higher in the case of DW than in the case of CS for all SAPs, a behaviour which is in accordance with literature [1].

Nevertheless, significant differences were observed among the three different SAPs. In both DW and CS the highest AR value was obtained by P(MAA-co-EGDMA)@SiO<sub>2</sub> and reached 3900 gg<sup>-1</sup> and 1920 gg<sup>-1</sup>, respectively, while the corresponding values for P(MAA-co-EGDMA) was determined at 515 and 511 gg<sup>-1</sup>, respectively.

### 3 Conclusions

In this work, hybrid organic-inorganic SAPs were synthesized and the effect of the (i) presence of ions and (ii) pH of different mediums on their water absorption were investigated. It was shown that the SAPs water absorption ratio was greatly increased after their modification with NaOH for both DW and CS due to the enhanced ionic nature of the molecules and their ability to participate in energy favourable ion-dipole interactions with water. This behavior was maintained and was even improved after their encapsulation in the SiO<sub>2</sub> shell for both DW and CS. Moreover, as shown in SEM pictures, after the water absorbance tests in both mediums hybrid SAPs maintained their structure while the structure of the SAPs before their encapsulation deteriorated. The combination of these properties with the enhanced chemical affinity between the hybrid SAPs and cement due to their inorganic SiO<sub>2</sub> shell promotes their use as additives in concrete to limit cracking during cement setting and hardening due to the gradual release of water absorbed by them and also limit the formation of macropores due the SAPs small size.

These results are part of a project that has received funding from the European Union's Horizon 2020 research and innovation program under grant agreement N°685445 (LORCENIS)

### References

1. A. Pourjavadi, M. Kurdtabar, G. R. Mahdavinia and Hossein, *Polymer Bulletin*, **57**, pp. 813-824 (2006).
2. A. Karatzas, P. Bilalis, I. A. Kartsonakis and G. C. Kordas, *Journal of Non-Crystalline Solids*, **358**, pp. 443-445 (2012).
3. D. Snoeck, D. Schaubroeck, P. Dubruel and N. De Belie, *Construction and Building Materials*, **72**, pp. 148-157 (2014).
4. M. Ebara et al., *Smart Biomaterials, NIMS Monographs, Chapter 2: Smart Hydrogels*, (Springer Japan, 2014).
5. E. M. Ahmed, *Journal of Advanced Research*, **6**, pp. 105-121 (2015).
6. A. Mignon, D. Snoeck, P. Dubruel, S.V. Vlierberghe and N. De Belie, *Materials*, **10**, 237 (2017).
7. H. Huang, G. Ye, C. Qian, E. Schlangen, *Materials and Design*, **92**, pp. 499-511 (2016).
8. V. Mechterine, *RILEM Technical Letters*, **1**, pp. 81-87 (2016).
9. J.Y. Wanga, D. Snoeck, S. Van Vlierberghe, W. Verstraete, N. De Belie, *Construction and Building Materials*, **68**, pp. 110-119 (2014).
10. N. Cao, X. Xie, Y. Zhang, Y. Zhao, L. Cao and L. Sun, *Journal of Industrial and Engineering Chemistry*, **34**, pp. 9-13 (2016).
11. A. Imtiaz, M.A. Farrukh, M. Khaleeq-ur-rahman, and R. Adnan, *The ScientificWorld Journal*, **2013**, pp. 1-11 (2013).
12. R. Zhanga, T. Shanga, G. Yanga, X. Jiaa, Q. Caia, X. Yanga, *Colloids and Surfaces B: Biointerfaces*, **144**, pp. 238-249 (2016).